cages. The current investigation probes the local geometry of the sodalite cage in detail, at the expense of longer range interactions such as pseudo-modeling energy contributions inherent to different frameworks composed of sodalite cages.

Acknowledgment. We greatly acknowledge the helpful interactions and discussions with Dr. Stelian Grigoras of Dow Corning Corp. and Dr. H. W. W. Tsao, and his colleagues, at Sun Refining and Marketing Co.

Properties of Atoms in Molecules: Atomic Volumes

Richard F. W. Bader,* Marshall T. Carroll, James R. Cheeseman, and Cheng Chang

Contribution from the Department of Chemistry, McMaster University, Hamilton, Ontario, Canada L8S 4M1. *Received May 1, 1987*

Abstract: The theory of atoms in molecules defines an atom and the average values of its properties. The intersection of an atomic surface, as defined by a property of the charge density, with a particular envelope of the charge density defines the volume of an atom in a molecule. The value of the density envelope used to bound the "open" portion of an atomic region can be chosen on the basis of comparison with measured properties. The nature of the results are, in any event, independent of the choice for envelopes which contain over 96% of the total electronic charge and lie within the usual range of van der Waals contact distances. It is shown that the volumes of methyl and methylene groups in normal hydrocarbons are transferable properties, as are their charge distributions, populations, and energies. The volume of a carbon atom subject to steric crowding is found to decrease as its stability and electron population increase. This behavior is opposite to that found for a carbon atom in a system with geometric strain as found in cyclic and bicyclic molecules. The stability, population, and volume of a carbon atom all undergo parallel increases as the atom is subjected to an increasing degree of geometric strain. The volumes of the bridgehead carbon atoms in bicyclo[1.1.0]butane and [1.1.1]propellane are 1.2 and 1.5 times, respectively, the volume of a methyl carbon atom. As anticipated on the basis of the orbital model, an increase in geometric strain is correlated with an increase in s character and thus one finds the electron population, stability, and volume of a carbon atom to undergo the same parallel increases in value through the series ethane, ethylene, acetylene. As a first step in the investigation of how atoms fit together, the changes in the atomic volumes accompanying the formation of a hydrogen bond are determined. The changes in volume are correlated with the changes in the atomic populations and energies for the formation of homo and hetero dimers of water and ammonia and their protonated species.

I. Introduction

It was pointed out by Bragg in 1920[1] that one can model a crystal through a representation of its atoms by spheres with characteristic radii, the radii being determined empirically from a body of experimental measurements so that the spheres of bonded atoms will be in approximate contact. This observation was followed by the establishment of sets of atomic (ionic) radii by a number of workers—Goldschmidt, Pauling, Zachariasen, and Slater as outlined in Slater's book on solids.[2] The idea of representing the spatial structure and extent of a system by centering "atomic" spheres of fixed radii at the experimentally determined average positions of the nuclei has been extended to systems other than crystals and is used for purposes other than accounting for or predicting crystal structures. Properties that one attempts to determine using the "atomic hard-sphere model" are the shape of a molecule, the volume it occupies, and the associated surface area. Bondi[3,4] calls the volume occupied by a molecule, that is, the volume impenetrable to other molecules, the van der Waals volume and the corresponding radii of the atomic spheres the van der Waals radii. The radii determined by van der Waals contact distances between molecules as required to recover packing densities of liquids and solids, kinetic collision cross sections, and other properties of the liquid state[3,4] result in spheres which overlap one another for neighboring atoms. Numerous algorithms have been proposed which take the common volume of overlapping atomic spheres into account in the calculation of the molecular volume. The scheme proposed by Gavezzotti[5] has been used to calculate the volumes of cavities in cage compounds and crystalline matrices and in the analysis of steric factors influencing reactions in the solid state.

The hard-sphere model has been useful in determining permissible peptide chain conformations.[6] Richards[7] has used the hard-sphere model to consider the packing of groups of atoms in proteins and the area of solvent-protein interfaces. The shape and area of the exposed surface of a molecule vary with the dimensions of the molecule used to probe its surface, reaching a limiting value as the size of the probe increases. Because of this problem, Richards has distinguished between the van der Waals envelope, the outer surface as determined by the hard-sphere model, the accessible surface, the continuous sheet defined by the locus of the center of the probe molecule as it rides over the van der Waals surface, the contact surface, those parts of the van der Waals surface that are actually in contact with the surface of the probe, and the reentrant surface, as defined by the interior facing part of the probe when it is simultaneously in contact with more than one atom. The latter two surfaces combine to form a continuous sheet which is a possible definition of the molecular surface, a surface termed the solvent-accessible surface by Connolly.[8] This author calculates the solvent-excluded volume of a molecule by a direct determination of the volume enclosed by the solvent-accessible surface, the surface, and its area being determined by an analytical procedure. This method is more accurate than previous ones because of its analytical treatment of the surface

(1) Bragg, W. L. *Phil. Mag.* **1920**, *40*, 169.
(2) Slater, J. C. *Quantum Theory of Molecules and solids*; McGraw-Hill: New York, 1925; Vol. 2, p 95.
(3) Bondi, A. *J. Phys. Chem.* **1964**, *68*, 441 (1964).
(4) Bondi, A. *Physical Properties of Molecular Crystals, Liquids and Glasses*; Wiley: New York, 1968.
(5) Gavezzotti, A. *J. Am. Chem. Soc.* **1983**, *105*, 5220; **1985**, *107*, 962.
(6) Ramachandran, G. N.; Sasisekharan, V. *Adv. Protein Chem.* **1968**, *23*, 284.
(7) Richards, F. M. *Annu. Rev. Biophys. Bioeng.* **1977**, *6*, 151.
(8) Connolly, M. L. *Science* **1983**, 221, 709; *J. Am. Chem. Soc.* **1985**, *107*, 1118.

0002-7863/87/1509-7968$01.50/0

and its area and because it avoids the problem of accounting for second- and higher-order overlaps of the atomic spheres.

The van der Waals volume will necessarily be less than the volume per molecule as determined by the experimentally determined molar volume at any temperature, thereby leading to the concept of a free volume as the difference between the two. Meyer et al.[9] have established procedures for scaling the radii of the mantel or outer atoms in such a way that the calculated molecular volume, termed the reduced molecular volume, approaches the experimental volume. The reduced molecular volume and its associated area, as well as providing correlations with various packing related properties and enthalpies of vaporization of liquids, is also used in the determination of cross-sectional areas as required in the analysis of adsorption isotherms.[9]

All of the above are based on the hard-sphere model of an atom. In 1967 Bader et al.,[10] in a study of the Hartree–Fock charge distributions of the second-row homonuclear diatomic molecules, demonstrated that an outer contour of the charge density could be used to assign a size and a shape to a molecule for its nonbonded interactions with other molecules, that is, define the van der Waals envelope. It was shown that the 0.002-au contour (1.000 au = 6.748 e/Å^3) yielded dimensions for the N_2 and O_2 molecules that were in reasonable agreement with diameters determined from kinetic theory data using the two-parameter potential of Kihara and Corner. A molecular shape as provided by the 0.002-au contour was used by Barrett et al.[11] in arriving at the packing of O_2 molecules in the α phase of the solid and by Mills and coworkers[12] in corresponding studies of a number of phases of solid N_2 and in discussions of possible structures of both molecular solids under high pressure.[13]

It is the purpose of this paper to further pursue the idea of using the charge distribution to determine the shapes and volumes of molecules. Since the initial investigation of this possibility in 1967, the theory of atoms in molecules has been developed,[14-17] and it is the elements of this theory that contribute to extending the use of the charge distribution in the determination of the size and shape of a molecule.

The definitions of an atom in a molecule, of the average values of its observables, and of their equations of motion are obtained through a generalization of quantum mechanics to a subsystem of some total system. This generalization is unique as it applies only to regions of real space that satisfy a particular constraint on the variation of the action integral, a constraint that is satisfied if the subsystem is bounded by a surface through which the flux in the gradient vector field of the charge density is zero

$$\nabla\rho\cdot n = 0 \qquad (1)$$

for every point on the surface. Because of the principal topological property of a charge distribution for a many-electron system (that it exhibits maxima only at the positions of nuclei), the quantum boundary condition eq 1 yields a partitioning of the real space of a molecule into a disjoint set of mononuclear regions or atoms. Atoms and functional groupings of atoms are illustrated in Figure 1 for two normal hydrocarbons. The intersections of the atomic surface of zero flux with the plane of the diagram are shown together with the bond paths, the paths which mark the presence of lines linking bonded nuclei along which the charge density is a maximum with respect to any neighboring line. These atoms

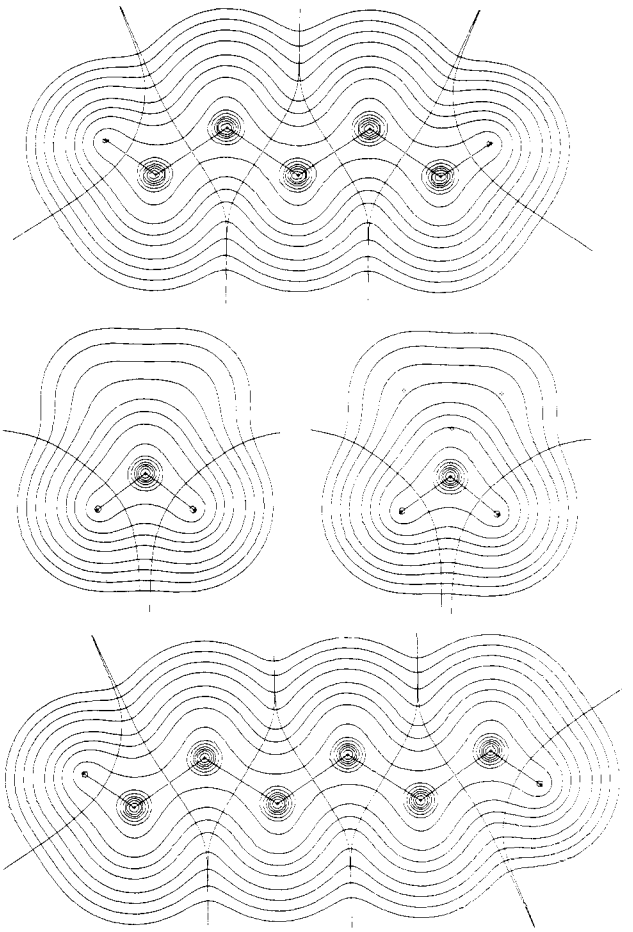

Figure 1. Contour maps of the charge density in pentane and hexane showing the bond paths and interatomic surfaces. (Contour values are given in Figure 3.) The maps make clear that the union of the interatomic surfaces and the outer density envelope bound an atomic region. The two middle maps are displays of the central methylene group in pentane (lhs) and of one of the two such groups in hexane (rhs) in a plane perpendicular to the plane containing the chain of carbon nuclei as displayed in the upper and lower maps. These two methylene groups possess identical properties and they are interchangeable between the two molecules, as are the methyl groups.

are the atoms of chemistry for their properties recover the measurable properties of atoms in molecules, properties such as the additive contribution of the methyl and methylene groups to the enthalpy of formation and the changes in these additive contributions to give the measured strain energies.[18-20]

Additivity and transferability of functional group properties are matters of importance to the present study. The atoms of theory exhibit properties essential to the existence of additivity schemes; they are the most transferable pieces of a system that can be defined in real space. All of the average properties of an atom are defined by quantum mechanics[21] with the average value of an observable $\hat{M}$ for the total system being given by the sum of the corresponding atomic averages $M(\Omega)$

$$\langle\hat{M}\rangle = \sum_\Omega M(\Omega) \qquad (2)$$

and, finally, the constancy in the properties of an atom, including its contribution to the total energy of a system, is observed to be directly determined by the constancy in its distribution of charge.

(9) Meyer, A. Y. *J. Mol. Struct.* **1985**, *124*, 93. Meyer, A. Y., Farin, D.; Avnir, D. *J. Am. Chem. Soc.* **1986**, *108*, 7897. Meyer, A. Y. *J. Comput. Chem.* **1986**, *7*, 144. Meyer, A. Y. *Chem. Soc. Rev.* **1986**, *15*, 449.

(10) Bader, R. F. W.; Henneker, W. H.; Cade, P. E. *J. Chem. Phys.* **1967**, *46*, 3341.

(11) Barrett, C. S.; Meyer, L. *Phys. Rev.* **1967**, *160*, 694. Barrett, C. S.; Meyer, L.; Wasserman, J. *J. Chem. Phys.* **1967**, *47*, 595.

(12) Schuch, A. F.; Mills, R. L. *J. Chem. Phys.* **1970**, *52*, 6000.

(13) Raich, J. C.; Mills, R. L. *J. Chem. Phys.* **1971**, *55*, 1811. Mills, R. L.; Schuch, A. F. *Phys. Rev. Lett.* **1969**, *23*, 1154. Schiferl, D.; Cromer, D. T.; Schwalbe, L. A.; Mills, R. L. *Acta Crystallogr., Sect. B* **1983**, *39*, 153.

(14) Bader, R. F. W.; Beddall, P. M. *J. Chem. Phys.* **1972**, *56*, 3320.

(15) Bader, R. F. W.; Nguyen-Dang, T. T.; Tal, Y. *Rep. Prog. Phys.* **1981**, *44*, 893.

(16) Bader, R. F. W.; Nguyen-Dang, T. T. *Adv. Quantum Chem.* **1981**, *14*, 63.

(17) Bader, R. F. W. *Acc. Chem. Res.* **1985**, *9*, 18.

(18) Wiberg, K. B.; Bader, R. F. W.; Lau, C. D. H. *J. Am. Chem. Soc.* **1987**, *109*, 985.

(19) Wiberg, K. B.; Bader, R. F. W.; Lau, C. D. H. *J. Am. Chem. Soc.* **1987**, *109*, 1001.

(20) Bader, R. F. W.; Larouche, A.; Gatti, C.; Carroll, M. T.; MacDougall, P. J.; Wiberg, K. B. *J. Chem. Phys.* **1987**, *87*, 1142.

(21) Included among these properties is the total electronic energy of an atom as defined by the virial theorem, $E(\Omega) = -T(\Omega) = T(\Omega) + V(\Omega)$, where T is the kinetic energy and V, the potential energy, is given by the virial of the forces exerted on the electrons.

When the distribution of charge over an atom is the same in two different molecules, i.e., when the atom or some functional groupings of atoms is the same in the real space of two systems, then it makes the same contributions to the total energy and other properties of both systems. It is because of the direct relationship between the spatial form of an atom and its properties that we are able to identify them in different systems. This paper demonstrates that the atomic volumes are another property that can be transferred essentially without change in normal hydrocarbons. The fact that the atoms of theory maximize the transfer of information between molecules at the level of the charge density is very important. Clearly, if the proposal to use properties of charge distributions to determine sizes and shapes of molecules is to be applicable to biological molecules, then one must demonstrate that it is possible to construct the charge distributions of large molecules, or their relevant portions, from the distributions of the fragments that serve as the building blocks for these large systems.

In an early study, nonbonded and bonded atomic radii were used to characterize the properties of charge distributions.[22] These radii[10] are respectively the distances of the nucleus from the 0.002-au contour on its nonbonded side and from the bond critical point on its bonded side (the point where the charge density attains its minimum value along the bond path), both measured along the internuclear axis. The value of the charge density at the bond critical point was also tabulated in this study for a large number of near-Hartree–Fock charge distributions for diatomic molecules. These parameters distinguished between ionic, polar, and covalent bonding. In ionic molecules, for example, the nonbonded radii were those of the corresponding free ions. The importance of dipolar polarizations of atoms in molecules where the donor atom has a number of valence electrons in excess of the number of holes present on the acceptor was demonstrated through examples such as CO and CN- where it is found that the nonbonded radius of carbon is 0.14 and 0.33 au greater, respectively, than the free atom value. In the present study, measurements of atomic size are related to mechanical properties of the atom to obtain a better understanding of the relationship of the size and shape of an atom in a molecule to its energy and charge.

Francl et al.[23] have studied the possibility of obtaining best atomic sphere radii fits to calculated charge distributions. Such a method suffers from the same problems as does the hard-sphere model in that it fails to reproduce the important features of the charge density that cannot be modelled by spherical atoms. These include obvious features such as the dipolar polarizations mentioned above and less obvious ones such as the observation reported here that a methylene group subject to geometric strain, as found in cyclopropane, is actually larger than the standard transferable methylene group.

The theory of atoms in molecules enables one to determine the volume of every atom in a system and the changes in these volumes caused by a chemical reaction. The volume change can be correlated with changes in other atomic properties, changes in its electron population and energy being of particular importance. These ideas are illustrated through a study of the changes in the atomic volumes, populations, and energies encountered in the formation of hydrogen bonds.

II. Atomic Volumes

Comparison of Density Envelopes. An atomic surface is the union of some number of interatomic surfaces, there being one such surface for each bonded neighbor and, if the atom is not an interior atom, some portions which may be infinitely distant from the attractor. The latter, open portions of the atomic surface are replaced with a particular density envelope in the calculation of an atomic volume. Thus an atomic volume is defined to be a measure of the region of space enclosed by the intersection of the atomic surface of zero flux and a particular envelope of the charge density; see Figure 1. In this work atomic volumes are reported for both 0.001- and 0.002-au density envelopes. The program PROAIM for the determination of the properties of atoms in molecules has been previously described.[24] The atomic average of every property is obtained by the integration of a corresponding density distribution function over the basin of the atom. Since the interatomic surfaces are uniquely defined and the partitioning is disjoint, there is no question of, nor problem with the overlap of atoms in the calculation of their properties.

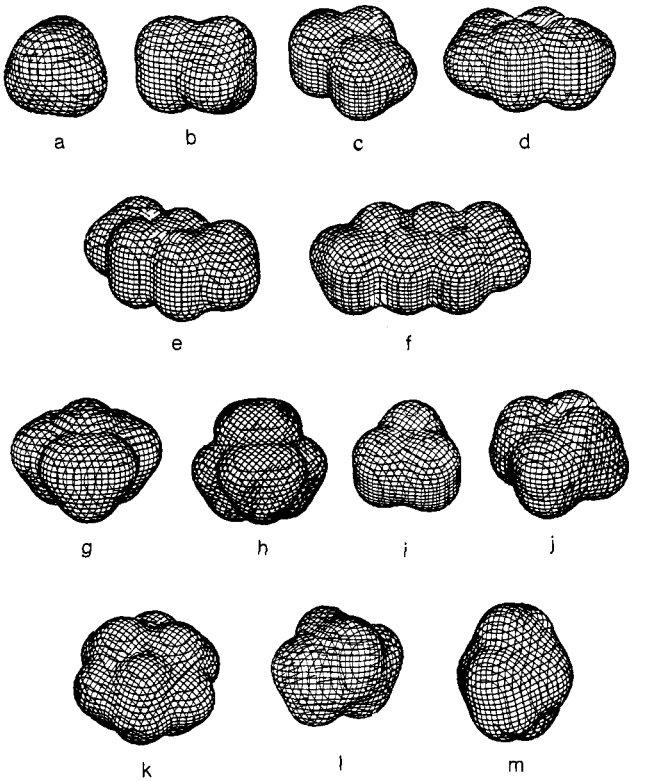

Figure 2. The 0.001-au density envelopes of hydrocarbon molecules. Their order in the diagram, a (methane) to m ([1.1.1]propellane), is the same as their order in Table II. The intersections of the zero flux interatomic surfaces with this envelope are readily drawn in by eye to yield the methyl and methylene groups of chemistry. The isobutane molecule, g, is three methyl groups, topped by a hydrogen atom.

The 0.001-au envelopes of some hydrocarbon molecules are illustrated in Figure 2. Table I lists the lengths and widths of these and other molecules as determined by both the 0.001- and 0.002-au envelopes and the averages of these values. All results are from state functions calculated using the 6-31G** basis using either 6-31G** or 6-31G* optimized geometries. In the cases of linear and symmetric top molecules the lengths and widths are taken as the two extremes of length along perpendicular axes. Appeal to the envelopes shown in Figure 2 for isobutane and neopentane, a spherical top, illustrate that the choices are in most cases obvious. For an asymmetric top molecule the maximum lengths along three orthogonal axes are given in Table I. It has previously been shown[25] that the 0.001-au contour for methane and the inert gases gives good agreement with the equilibrium diameters of these molecules as determined by second virial coefficient or viscosity data fitted with a Lennard-Jones 6–12 potential.[26] The experimental values of σ, the Lennard-Jones

(22) Bader, R. F. W.; Beddall, P. M.; Cade, P. E. *J. Am. Chem. Soc.* **1971**, *93*, 3095.

(23) Francl, M. M.; Hout, R. F.; Hehre, W. J. *J. Am. Chem. Soc.* **1984**, *106*, 563.

(24) Biegler-König, F. W.; Bader, R. F. W.; Tang, T. H. *J. Comput. Chem.* **1982**, *3*, 317. The integration program PROAIM already contains procedures for integrating properties over an interatomic surface. The same procedure could be adapted to measure the area of the contribution of each atom to the density envelope and in this manner determine the area of the van der Waals surface.

(25) Bader, R. W. F.; Preston, H. J. T. *Theor. Chim. Acta* **1970**, *17*, 384.

(26) The Lennard-Jones 6–12 potential $U(r)$ equals zero for r equal to σ, the collision diameter, and it equals the well depth $-\epsilon$ for r equal to the equilibrium separation $2^{1/6}\sigma$.

Table I. Sizes and Volumes of Molecules as Determined by Density Envelopes

	0.001-au envelope, au			0.002-au envelope, au				V_M, cm³/mol		V_M/V_m[a] 0.001	
	length	width	av	length	width	av	$2^{1/6}\sigma$[a]	0.001	0.002		
ethane	10.0	8.4		9.4	7.6		8.27	39.54	31.10	0.72	T_b
propane	13.4	9.1		12.8	8.2		9.12	53.64	42.76	0.71	T_b
butane	15.8	9.1		15.3	8.2		9.12	67.64	44.13	0.70	T_b
pentane	18.3	9.1		17.7	8.2			81.56	65.96	0.75	T_r
hexane	20.6	9.1		20.0	8.2			95.71	72.49	0.73	T_r
isobutane	12.4	10.0	11.2	11.6	9.8	10.7	10.60	67.21	54.53		
neopentane	12.6	12.6	12.7	12.2	12.2	12.2	13.15	80.78	65.95	0.66	T_r
cyclopropane	10.3	8.6	9.4	9.6	8.0	8.8	8.97	45.85	36.69		
cyclohexane	14.6	10.4	12.5	13.9	10.1	12.0	12.73	84.70	69.35	0.80	T_b
methane	8.2	8.2	8.2	7.3	7.3	7.3	8.06	25.53	19.58	0.72	T_m
H_2	6.4	6.0	6.2	5.8	5.4	5.6	6.13	10.75	7.78		
N_2	8.8	7.0	7.9	8.3	6.7	7.5	7.72	20.61	16.68	0.64	T_m
O_2	8.4	6.5	7.5	7.9	5.9	6.9	7.34	18.28	14.93	0.75	T_m
Ne	5.8	5.8	5.8	5.4	5.4	5.4	5.83	8.70	6.75	0.21	T_c
Ar	7.5	7.5	7.5	6.9	6.9	6.9	7.21	19.10	15.49	0.26	T_c
C_2H_4	10.0	8.6	8.8	9.3	8.0	8.1	8.27	25.46	20.45	0.52	T_b
		7.8			7.1						
C_2H_2	10.9	7.7	9.3	7.0	10.4	8.7	7.00	36.37	28.70	0.86	T_b
F_2	8.3	6.5	7.4	7.9	5.9	6.9	6.90	17.18	14.04	0.50	T_b
NO	8.6	6.8	7.7	8.1	6.2	7.1	6.72	20.78	15.45	0.92	T_m
HF	6.7	6.1	6.4	6.2	5.7	6.0		10.90	8.91	0.54	T_r
CO	8.9	6.8	7.9	8.5	6.2	7.3	7.11	21.10	16.62	0.60	T_m
NH_3	7.8	7.5	7.6	7.2	6.9	7.0	6.41	20.20	15.88	0.76	T_r
H_2O	6.7	7.4	7.0	6.3	7.1	6.6	5.81	15.63	12.54	0.87	T_r
		6.8			6.3						
PH_3	9.5	8.9	9.2	8.8	8.2	8.5		33.95	26.43	0.74	T_b
CO_2	10.7	6.7	8.7	10.2	6.5	8.3	7.21	25.88	21.20	0.69	T_0
SO_2	11.1	8.1	8.9	10.6	7.8	8.4	7.63	33.10	27.20	0.74	T_m
		7.4			6.7						
NNO	10.8	7.0	8.9	10.3	6.4	8.4	7.00	27.81	22.19	0.78	T_m
HCN	9.9	7.3	8.6	9.4	6.7	8.0		25.18	20.07	0.65	T_b
HCP	11.4	8.4	9.9	10.8	7.6	9.2		36.66	29.78		
HCl	8.5	8.1	8.3	7.9	7.4	7.6	6.79	24.16	18.97	0.66	T_m

[a] Marcus, Y. *Introduction to Liquid State Chemistry*; Wiley: New York, 1977. Hirshfelder, J. O.; Curtis, C. F.; Bird, R. B. *Molecular Theory of Gases and Liquids*; Wiley: New York, 1954. *International Critical Tables*; McGraw-Hill: New York, 1927.

6–12 collision diameter, multiplied by $2^{1/6}$ to give the equilibrium separation between molecules are also tabulated. Unlike the work referred to earlier where the 0.002-au contour was used to determine the packing of N_2 and O_2 molecules in the (condensed) crystalline phase, the average diameters as determined by the 0.001-au envelope of the inert molecules CH_4 to Ar, molecules without dipolar polarizations, are in reasonable agreement with the experimental equilibrium separations as measured in the gas phase. The equilibrium separations of polar molecules are consistently less than the diameters determined by either the 0.001- or 0.002-au envelope. This observation is consistent with the decreases in molecular volumes which accompany the formation of a hydrogen bond as discussed and illustrated later in this paper.

The width listed for a normal alkane after C_2H_6 is the average of the two maximum widths of a methylene group for the plane illustrated in Figure 1, ignoring small indentations in the appropriate contour. This value is remarkably constant, a reflection of the transferable properties of the methylene group as will be further discussed and illustrated. This width is also in good agreement with the experimental equilibrium separation, indicating that in these cases the experiment is measuring the average cross-sectional diameter of the molecule and that the result is independent of its length.

The molecular volume v_M is obtained by summing the volumes of the constituent atoms, $v(\Omega)$. The molecular molar volume V_M is the value of v_M for 1 mole, and these values are compared with the experimentally measured molar volumes V_m in Table I. The ratio V_M/V_m is close to 0.7 for all of the normal alkanes. The ratio of occupied space to the total space required for random close packing of spheres is 0.64, while for a regular packed lattice this ratio is 0.74.[27] For the majority of other substances in Table I, V_M/V_m lies in the range 0.6 to 0.8 at their boiling point (T_b), melting point (T_m), or at room temperature (T_r). There is a dramatic decrease in this ratio for a system at its critical point (T_c).

The van der Waals radii of Gavezzotti[5] for carbon and hydrogen, which are very similar to those given earlier by Bondi,[3] provide a reasonable fit to the 0.002-au envelope of the methane and propane molecules as is evident from Figure 3. The values of V_M, however, differ significantly, Gavezzotti's algorithm yielding values of 16.9 and 37.0 cm³/mol, respectively, compared to the 0.002-au density envelope values of 19.6 and 42.8 cm³/mol. The discrepancy arises primarily from the departure of the outer envelope from the spherical shape of the atoms assumed in the model. Figures 2 and 3 make clear an observation also made by Francl et al.[23] that the surface defined by either the 0.001- or 0.002-au density envelope is smoother than that determined by the hard-sphere model. As indicated in Figure 3, the area of an outer-density envelope will, in general, yield a close approximation to the solvent-accessible surface if the probe molecule is assigned the usual value of 1.4 to 1.5 Å, the average diameter of a water molecule.[7]

The problems investigated in this paper were studied using both the 0.001- and 0.002-au density envelopes. The nature of the results is found to be independent of the choice of contour value for contours which are large enough to contain at least ~96% of the electronic charge and lie within the usual limits of van der Waals contact distances.

Atomic and Group Properties of Hydrocarbons. Table II lists the volume of each atom in hydrocarbon molecules, in normal and branched alkanes, in cyclic and bicyclic molecules, for unsaturated systems, and for some carbocations for both the 0.001- and 0.002-au envelopes. The energy and the electron population of each atom together with the fraction of this total population contained within the indicated envelope are also given. Table III gives the molecular molar volume and the contribution of each functional group to this volume. A check on the accuracy of the

(27) Marcus, Y. *Introduction to Liquid State Chemistry*; Wiley: New York, 1977; p 58.

Table II. Atomic Energies, Populations, and Volumes[a]

molecule	atom[b]	$-E(\Omega)$	$N(\Omega)$	$v(\Omega)$ 0.001	$v(\Omega)$ 0.002	% N(Ω) 0.001	% N(Ω) 0.002
CH_4	C	37.6097	5.754	76.90	64.94	99.7	99.4
	H	0.6480	1.062	52.31	38.61	97.8	96.0
C_2H_6	C	37.6328	5.762	64.66	57.90	99.8	99.6
	H	0.6621	1.079	52.30	38.79	98.0	96.1
C_3H_8	C	37.6502	5.774	63.45	57.31	99.9	99.7
	H	0.6615	1.079	52.44	38.87	98.0	96.1
	H	0.6625	1.082	52.59	39.45	98.1	96.4
	C	37.6539	5.778	54.75	51.37	98.0	97.9
	H	0.6744	1.092	52.10	38.83	98.0	96.3
C_4H_{10}	C	37.6470	5.773	63.36	57.29	99.9	99.7
	H	0.6622	1.079	52.38	38.80	97.9	96.2
	H	0.6632	1.083	52.52	39.44	98.1	96.3
	C	37.6695	5.791	53.79	50.72	99.9	99.9
	H	0.6750	1.095	52.20	39.43	98.2	96.6
C_5H_{12}	C	37.6469	5.773	63.64	57.30	99.9	99.7
	H	0.6621	1.080	52.37	38.85	97.9	96.1
	H	0.6629	1.082	52.41	39.49	98.1	96.4
	C	37.6716	5.791	53.64	50.69	99.9	99.9
	H	0.6747	1.095	52.09	39.38	98.2	96.6
	C	37.6910	5.803	52.36	49.98	100.0	99.9
	H	0.6753	1.098	52.13	40.03	98.3	96.8
C_6H_{14}	C	37.6480	5.775	63.57	57.29	99.9	99.7
	H	0.6615	1.079	52.40	38.89	97.9	96.1
	H	0.6627	1.082	52.59	39.44	98.1	96.3
	C	37.6707	5.790	53.60	50.65	99.9	99.9
	H	0.6751	1.095	52.16	39.42	98.3	96.6
	C	37.6884	5.804	52.76	50.30	100.0	99.9
	H	0.6756	1.098	52.21	39.99	98.4	96.8
iso-C_4H_{10}	C	37.6649	5.781	61.29	56.23	99.9	99.8
	H	0.6625	1.084	52.21	39.99	99.9	98.2
	H	0.6627	1.082	52.41	39.38	98.1	96.4
	C	37.6759	5.808	47.28	45.74	100.0	99.9
	H	0.6845	1.102	51.49	38.65	98.3	96.6
neo-C_5H_{12}	C	37.6746	5.786	59.75	55.25	99.9	99.8
	H	0.6634	1.084	52.10	39.76	98.3	96.6
	C	37.6938	5.851	40.97	40.97	100.0	100.0
C_3H_6	C	37.7115	5.894	70.84	62.11	99.8	99.6
	H	0.6557	1.053	50.21	37.47	97.9	96.2
C_4H_8	C	37.6905	5.830	60.83	55.34	99.9	99.7
	H	0.6683	1.086	52.64	38.93	98.0	96.2
	H axial	0.6686	1.084	52.12	38.66	98.1	96.3
C_6H_{12}	C	37.6896	5.809	53.70	50.67	99.9	99.9
	H	0.6729	1.092	52.25	38.85	98.0	96.3
	H axial	0.6754	1.099	52.24	39.99	98.3	96.7
bicyclo[1.1.0]butane	C	37.6702	5.814	68.14	59.62	99.8	99.6
	H axial	0.6577	1.062	51.49	38.51	98.1	96.3
	H	0.6557	1.055	50.72	37.54	97.9	96.1
	C	37.8253	6.061	78.69	68.22	99.8	99.5
	H	0.6322	1.009	48.05	36.10	97.8	96.1
[1.1.1]propellane	C	37.7330	5.864	65.86	58.08	99.8	99.6
	H	0.6494	1.033	48.39	36.83	98.2	96.5
	C	37.8041	6.102	93.77	76.83	99.7	99.2
C_2H_4	C	37.7250	5.919	92.37	77.27	99.6	99.3
	H	0.6473	1.041	50.30	37.31	97.8	96.0
C_2H_2	C	37.8418	6.121	121.06	98.46	99.4	98.8
	H	0.5691	0.879	41.35	31.18	97.7	96.1
CH_3^+	C	37.6826	5.757	95.46	77.01	99.5	99.0
	H	0.5179	0.748	35.70	26.61	97.5	95.8
$C_4H_9^+$	C	37.7136	5.796	68.22	60.39	99.8	99.6
	H[c]	0.6170	0.969	45.18	34.91	98.1	96.6
	H	0.5896	0.934	44.53	34.21	97.9	96.4
	C	37.9288	6.099	64.58	60.21	99.9	99.8

[a] All results in atomic units and calculated from 6-31G**/6-31G*. [b] The carbon atom of a methyl group, if present, is listed first. This is followed by the unique H of a methyl and then by one of the two equivalent hydrogens of a methyl. Given next are the carbon and hydrogen atoms of methylene. The final entries are for carbon and hydrogen of methine and finally a single carbon as in neopentane. [c] In plane.

integrations is also given by the listing of the difference between the sum of the total atomic populations and the total number of electrons in the molecule.

The study of the molar volumes of the normal alkanes provided the earliest example of the additivity of group properties.[28] The experimentally determined heats of formation of the same series of molecules also obey a group additivity scheme.[29-31] This additivity is mirrored by the single determinant SCF energies at

(28) Kopp, H. (1855), as reported in: Glasstone, S. *Textbook of Physical Chemistry*, 2nd ed.; Van Nostrand; New York, 1946; p 525.

(29) Franklin, J. L. *Ind. Eng. Chem.* **1949**, *41*, 1070.

(30) Prosen, E. J.; Johnson, W. H.; Rossini, F. D. *J. Res. Natl. Bur. Stand.* **1946**, *37*, 51.

(31) Pittam, D. A.; Pilcher, G. *J. Chem. Soc., Faraday Trans.* **1972**, *1*, 68, 2224.

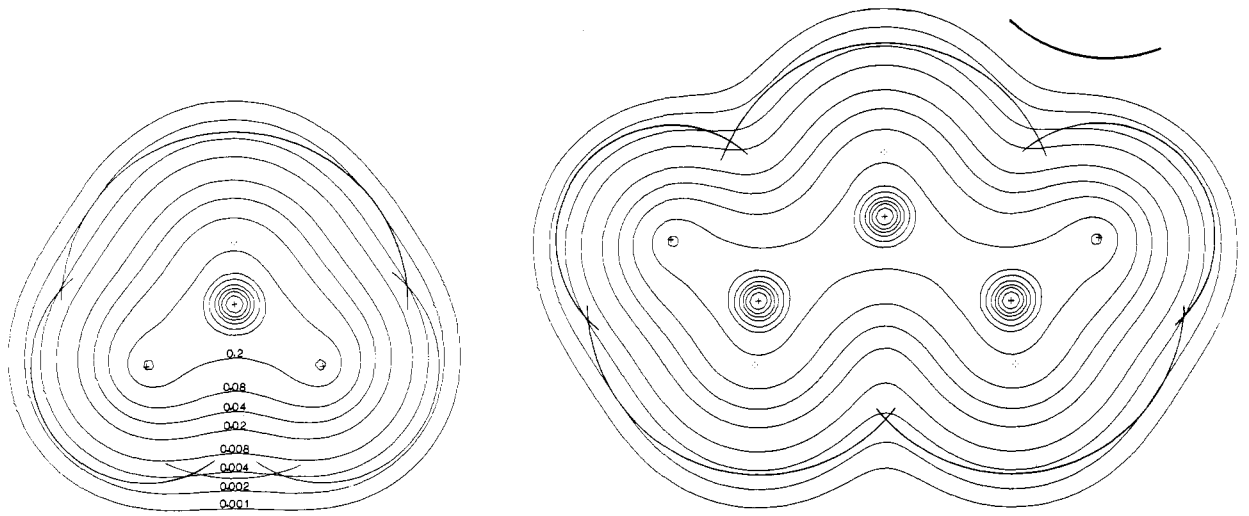

Figure 3. Contour maps (contour values are in au) of methane and propane overlaid with spherical boundaries centered at the hydrogen and carbon nuclei with radii equal to van der Waals values of 2.21 au for H and 3.31 au for C.[5] The arc is a portion of a sphere used to represent a water molecule, with a radius of 2.74 au ≡ 1.45 Å.[7]

both the 6-31G*/6-31G* and 6-31G**/6-31G* levels of approximation.[19,32,33] The calculated molecular energies E for the alkanes $CH_3(CH_2)_mCH_3$, including $m = 0$, satisfy the relationship

$$E = 2E(CH_3) + mE(CH_2) \quad (3)$$

$E(CH_3)$ is one-half the energy of ethane, equal to −39.61912 au, and $E(CH_2)$ is the energy increment per methylene group equal to −39.03779 ± 0.00014 au, with an error less than the experimental ones. The energy values are for the 6-31G**/6-31G* results. All properties of the methyl and methylene groups in this homologous series exhibit the same pattern of transferable values as do their energies and populations. The group contributions to these two important properties are briefly reviewed to provide an understanding of the properties of the group volumes.

Hydrogen is slightly more electronegative than carbon in saturated hydrocarbons, and the order of the group electron-withdrawing ability in hydrocarbon molecules without geometric strain is $H > CH_3 > CH_2 > CH > C$.[19,32] In ethane, methyl is bonded to methyl while in the other molecules of the series it is bonded to methylene from which it withdraws charge. However, to within the accuracy of the numerical integrations (which in general are ±0.001 e and ±1.5 kcal/mol), the energy and population of the methyl group are constant when it is bonded to a methylene group. Thus the CH_3 group is the same in all of the members of the homologous series past ethane. This transferable methyl group is more stable relative to methyl in ethane by an amount $\Delta E = -10.5 \pm 0.5$ kcal/mol, and its electron population is greater by an amount $\Delta N = 0.0175 \pm 0.0005$ e.[19,20,32]

The charge and energy gained by the methyl group is taken from the methylene group. What is remarkable, and what accounts for the additivity observed in this series of molecules, is that the energy gained by methyl is equal to the energy lost by methylene. In propane, where methylene is bonded to two methyls, its energy relative to the increment for methylene in eq 3 is $E(CH_2) - 2\Delta E$, and its net charge is $+2\Delta N$ where ΔE and ΔN are identical with the quantities defined above for methyl. In butane, a methylene is bonded to a single methyl; its energy is $E(CH_2) - \Delta E$ and its charge is $+\Delta N$. The corresponding groups in pentane and hexane, those bonded to a single methyl (see Figure 1), have the same properties as the methylene group in butane. Thus the charge transfer to methyl is damped by a single methylene group, and the central methylene group in pentane and the two such groups in hexane (see Figure 1) should have a zero net charge and an energy equal to the increment $E(CH_2)$. This is what is

Table III. Molecular Molar Volumes of Molecule and Functional Group

molecule and group	V_M, cm³/mol 0.001	0.002	$N - \sum_\Omega N(\Omega)$
CH_4	25.53	19.58	+0.0003
CH_3	20.87	16.13	
C_2H_6	39.54	31.10	+0.0006
CH_3	19.77	15.55	
C_3H_8	53.64	42.76	+0.002
CH_3	19.73	15.62	
CH_2	14.18	11.51	
C_4H_{10}	67.64	44.13	+0.002
CH_3	19.70	15.61	
CH_2	14.12	11.56	
C_5H_{12}	81.56	65.96	+0.004
CH_3	19.71	15.63	
CH_2	14.08	11.55	
CH_2[a]	13.98	11.61	
C_6H_{14}	95.71	72.49	+0.003
CH_3	19.74	15.62	
CH_2	14.09	11.56	
CH_2[a]	14.03	11.63	
i-C_4H_{10}	67.34	54.36	−0.002
CH_3	19.51	15.61	
CH	8.81	7.53	
neo-C_5H_{12}	80.78	65.95	+0.002
CH_3	19.28	15.57	
C	3.66	3.66	
C_3H_6	45.85	36.69	+0.002
CH_2	15.28	12.23	
C_4H_8	59.11	47.45	+0.001
CH_2	14.78	11.86	
C_6H_{12}	84.25	69.35	+0.002
CH_2	14.04	11.53	
bicyclo[1.1.0]butane	53.02	42.83	+0.001
CH_2	15.20	12.02	
CH	11.31	9.31	
[1.1.1]propellane	60.28	48.98	+0.002
CH_2	14.51	11.76	
C	8.37	6.86	
C_2H_4	34.44	27.11	−0.00007
CH_2	17.22	13.56	
C_2H_2	28.99	23.24	+0.00006
CH	14.49	11.62	
CH_3^+	18.14	14.00	−0.001
$C_4H_9^+$	59.97	49.19	+0.002
CH_3	18.07	14.61	
C	5.76	5.37	

[a] These methylenes are bonded only to other methylenes.

(32) Bader, R. F. W. *Can. J. Chem.* **1986**, *64*, 1036.
(33) The group zero-point energy corrections are additive for the *n*-alkanes (Schulman, J. M.; Disch, R. L. *Chem. Phys. Lett.* **1985**, *113*, 291) as are the group enthalpy corrections from 0 to 298 K (Wilberg, K. B. *J. Comput. Chem.* **1984**, *5*, 197).

found to within the uncertainties in the integrated values of the atomic properties, their calculated net charges being 0.0005 ± 0.0002 and their energies deviating from the standard value by 1.5 ± 0.5 kcal/mol. Therefore, methylene groups bonded only to other methylenes, as found in pentane, hexane, and all succeeding members of the series, possess a zero net charge and contribute the standard increment $E(CH_2)$ to the total energy of the molecule. The underlying reason for the observation of additivity in this series of molecules is the fact that the change in energy for a change in population, the quantity $\Delta E/\Delta N$, is the same for both the methyl and methylene groups. The small amount of charge shifted from methylene to methyl makes the same contribution to the total energy.

It is to be emphasized that the energies assigned to the methyl and methylene groups are independently determined by the theory of atoms in molecules. The fact that this assignment leads to an energy for the transferable methylene group equal to the value $E(CH_2)$ as determined by the total energies in eq 3 confirms that these atoms are the atoms of chemistry. *The properties of atoms in molecules can be measured experimentally, the methylene increment to the heats of formation being an example, and quantum mechanics predicts these properties as it does the properties of the total molecule.*

The volumes of the methyl and methylene groups in this homologous series of hydrocarbons listed in Table III reflect the same pattern of transferable values. The volume of the methyl group in ethane is slightly larger than that of the methyl groups in the remaining members whose volumes vary by only ±0.02 au from their average value. The volume of the methylene group bonded to two methyls in propane is slightly greater than the volumes of the methylene bonded to one methyl, their volumes varying by ±0.02 au about the average value. Finally, the methylene groups bonded only to other methylenes also have a characteristic volume. The small differences between the latter two kinds of methylene groups are evident in Figure 1. The methylene bonded to one methyl is less compressed than one bonded only to other methylenes and this is reflected in its larger volume. This effect is enhanced for propane where the single methylene is larger still. The volume varies in the reverse order to the population and energy of the methylene group: the more contracted the group, the larger its population and the lower its energy. The same is true for the methyl group, the transferable methyl having a smaller volume, but larger population and lower energy than the methyl of ethane. It has also been shown[20] that the methyl and methylene group dipole moments and their correlation energies as determined by a density functional exhibit the identical pattern of transferable values.

The methyl groups in isobutane and neopentane have still larger net charges and still lower energies since they withdraw charge from CH and C, respectively. Correspondingly they have smaller volumes, the smallest being found for the most stable, that in neopentane. One notes that the volume and contained charge of the central carbon in this latter molecule is independent of the choice of envelope as it is interior to both the 0.001- or 0.002-au contour. This observation is borne out by the fact that both choices of envelope recover 100% of the charge of this atom. The stability and electron population of a carbon atom increases with the extent of methyl substitution, as methyl is less electron withdrawing than is hydrogen. The volume of a substituted carbon, however, exhibits the opposite order, its value decreasing in the order ethane > propane > isobutane > neopentane.

Consequences of Geometric Strain. What might at first seem surprising from the next entries in Table II and III is that the volume of a carbon atom increases as it is subjected to increased geometric strain. The extent of geometric strain present in a molecule is measured by comparing the bond path angle with the normal bond angle.[18] An example is given in Figure 4 which shows that the bond path angle of 78.8° in cyclopropane is considerably less than the normal tetrahedral CCC bond angle. The strain in this molecule is, however, less than that suggested by the geometric angle which is less than the bond path angle by 18.8°. The strain is still less in cyclobutane, and correspondingly the bond path angle

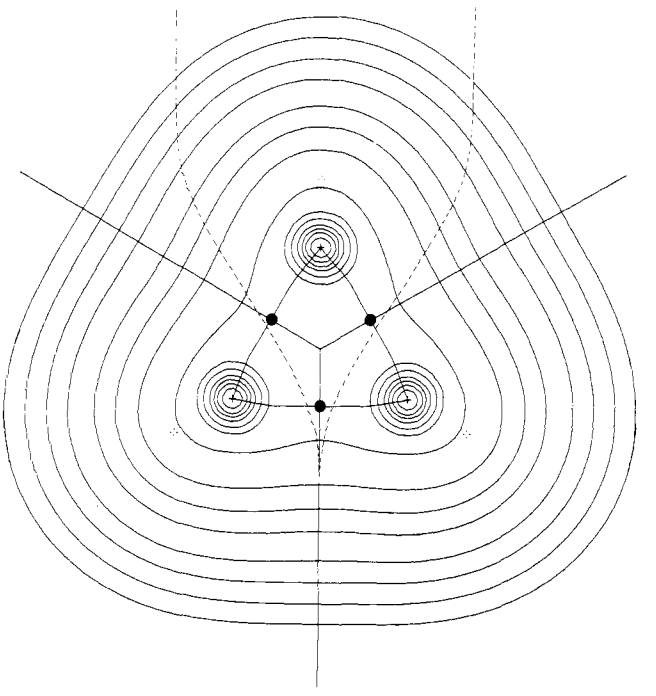

Figure 4. Contour map of cyclopropane in plane containing carbon nuclei. (Contour values are as given in Figure 3.) The carbon–carbon bond paths and the intersection of the carbon–carbon interatomic surfaces with this plane are also shown. The dots denote (3, −1) or bond critical points. The dashed lines denote the corresponding atomic boundary of the carbon atom in the transferable methylene group illustrated in Figure 1.

exceeds the geometric angle of 89.0° by only 6.7°. In the strain-free cyclohexane molecule the bond path angle is actually closer to the tetrahedral value than is the geometric one since the latter, equal to 111.4°, *exceeds* the former by 1.3°. Correspondingly, the volume of the carbon in cyclopropane is greater than that for the carbon in cyclobutane which in turn is greater than that for cyclohexane. Unlike the variation in volume of a carbon with extent of methyl substitution discussed above, one finds both the electron population and stability of a strained carbon to parallel the increase in its volume. These observations, together with an understanding of strain energy itself, can be rationalized in terms of orbital models of electronic structure.

The hybridization model predicts that the smaller bond angles found in hydrocarbons with angular strain should result in an increase in the p character of the strained C–C bonds and hence in an increase in the s character of the associated C–H bonds.[34,35] Orbital theories in turn predict the electronegativity and stability of a carbon to increase relative to that of its bonded hydrogen with an increase in s character, as s electrons are bound more tightly than are p electrons.[36] Thus as seen from the values in Table II for C_2H_6, C_2H_4, and C_2H_2, the stability and electron population of a carbon atom increase as its hybridization undergoes a corresponding change from sp^3 to sp^2 to sp. The increases in the electron population and stability of a carbon atom which are found to parallel the extent of geometric strain present in a cyclic system are similarly a consequence of an increasing s character. This paralleling behavior of charge, stability, and strain is reflected in the atomic populations and energies given in Table II and is more fully documented in a study of the atomic properties in a wide variety of hydrocarbons.[19] The atomic volume of carbon is another property whose value increases with increasing s character (the values of v(C) in ethane, ethylene, and acetylene being 65, 92, and 121 au, respectively) and also with increasing geometric strain.

(34) Coulson, C. A.; Moffit, W. E. *Phil. Mag.* **1949**, *40*, 1.
(35) Walsh, A. D. *Nature (Lond.)* **1947**, *159*, 167, 712.
(36) Coulson, C. A. *Valence*, 2nd ed.; Oxford University Press: Oxford, 1961; p 218.

The increase in stability, charge, and volume of a carbon atom with increasing geometric strain is illustrated by the results for the three cyclic molecules cyclohexane, cyclobutane, and cyclopropane. It is important to note that the theory of atoms in molecules again recovers the experimental findings regarding the values of the strain energies for these molecules. The energy of the methylene group in cyclohexane differs from the energy of the standard methylene group (a value fixed independently by the partitioning of the energies of the normal hydrocarbons) by only 0.06 kcal/mol. The charges of the carbon and hydrogen atoms in this group and in the transferable methylene group in pentane and hexane are also very similar. Thus in agreement with experiment, cyclohexane has a zero strain energy. The strain present in the four- and three-membered rings results in a transfer of charge from hydrogen to carbon relative to their values in the standard methylene group. The extent of this charge transfer increases with an increase in strain. The result is an increase in the stability of the carbon atom, but an even greater decrease in the stability of the two hydrogen atoms relative to their values in the standard methylene group and the net result is a strain energy. The strain energy per methylene group is greater for cyclopropane than for cyclobutane, the values being 9.3 and 6.5 kcal/mol, respectively. In agreement with experiment, the predicted total strain energies of 27.9 and 26.0 kcal/mol for the two molecules are very similar.

The volume changes for the hydrogens attached to the strained carbon atoms parallel the shifts in charge, their volumes being slightly less than the volumes of the hydrogen atoms in the standard methylene group. The increase in volume of the carbon atom dominates the volume change accompanying the introduction of geometric strain into a cyclic molecule. The reason for this can be seen from Figure 4 which shows the boundaries of the carbon atom of the standard methylene group superimposed on the carbon atom of cyclopropane in the plane of the carbon nuclei. The effect of decreasing the angle between the carbon–carbon bond paths subtended at the nucleus of the standard methylene carbon to its value in cyclopropane is a fan-like opening up of the carbon atom and a corresponding increase in its breadth. There is a loss in its relative volume where the boundaries of the three ring atoms meet, but this is small compared to the gain in the outer regions of the atom. It is also important to note that this result of an increase in volume of the methylene group with increase in strain is not an artifact of the partitioning method. Thus the incremental increase in the total molecular volumes, propane through to hexane, is 14.0 au. This increment per added methylene group is less than one-third and one-quarter respectively of the total molecular volumes of cyclopropane and cyclobutane. Gavezzotti[5] has noted that the surface area of a methylene group increases with geometric strain and decreases with steric crowding.

Also included in the tables are the results for bicyclo[1.1.0]-butane and [1.1.1]propellane. In both these molecules all four bonds to a bridgehead carbon atom lie on one side of a plane through its nucleus. In keeping with the considerable geometrical strain present at the bridgehead positions, these atoms are the most stable, and possess the largest net charges and volumes of all the saturated carbon atoms considered here. The bridgehead carbon in bicyclo[1.1.0]butane is over one and one-half times larger than the methine carbon in isobutane. It is only 10.4 kcal/mol less stable than the sp-hydridized carbon atom of acetylene with a net charge one-half as great, suggesting a considerable degree of s character in its bonds to neighboring groups from which it withdraws charge.[19] The volume of a bridgehead carbon in [1.1.1]propellane is nearly 50% larger than that of a methyl group carbon atom and more than twice as large as the central carbon in neopentane. One notes from the envelopes illustrated in Figure 2 that the bridgehead carbons are large and exposed in these two molecules. In keeping with this observation, both molecules undergo acetolysis by protonation of the bridgehead carbons, as previously discussed in more detail in terms of the Laplacian of the charge density.[18,19]

In the normal and branched alkanes the general behavior, as noted above, is for the volume of a carbon atom to decrease as its stability and electron population increase. This behavior is what is observed for atomic volumes of the free atoms across a short row of the periodic table, from an alkali metal to an inert gas. In the strained hydrocarbons, on the other hand, just the opposite behavior is observed, with the volume increasing along with an increase in population and stability of the carbon.

The parallel increases in electron population, stability, and volume of a carbon atom which accompany an increase in its s character is further illustrated by the series ethane, ethylene, and acetylene. The idea extends to carbocations as well (Tables II and III), the sp^2 carbons of CH_3^+ and $C(CH_3)_3^+$ having volumes in excess of those for an sp^3 carbon in the hydrocarbons from which they are derived. Correspondingly, they also have greater electronegativities as reflected in their net charges and stabilities. Thus the positive charge in CH_3^+ is shared equally over all four nuclei, and as anticipated in terms of the hyperconjugation model, the electron population of the central carbon increases with increasing methyl substitution, the central carbon in tertiary butyl carbon bearing a net negative charge.[32] While $v(C)$ is greater for the sp^2 carbon of a carbocation than it is for the corresponding carbon in the saturated hydrocarbon from which it is derived, the value of $v(C)$ for the sp^2 carbon is found to decrease, rather than increase, with $N(C)$. The width of an sp^2 carbon in the plane perpendicular to the plane of the nuclei does indeed increase with the increase in hyperconjugative electron release to this carbon which accompanies an increase in methyl substitution, from 5.7 au in CH_3^+ to 6.7 au in $C(CH_3)_3^+$. In the plane of the nuclei, however, the C of CH_3^+ extends between the H atoms while in $C(CH_3)_3^+$ the central carbon is totally enclosed by the interatomic surfaces with other carbons. In addition to the net charges on the carbon in CH_3^+ and in methane being the same, the former is more stable than the latter by 45.7 kcal/mol. The stability of the carbon which changes from sp^3 to sp^2 on formation of a carbocation increases with the extent of methyl substitution, equalling 147 kcal/mol in the case of *tert*-butyl cation, thereby accounting for the observation that the acidity of a branched hydrocarbon increases with the extent of methyl substitution.

The volume of a methylene group decreases along with a decrease in the number of adjacent methyl groups. This is evident in Figure 1 where the methylene carbon adjacent to the methyl carbon appears less confined than the one next to it which is bonded only to methylenic carbons. The volume of the carbon atom in a methyl group and of the group itself decrease as the number of methyl groups substituted on a single carbon increases. The volume of a carbon atom also decreases with the extent of methyl substitution. In all of these cases, the volume decrease of the carbon atom is accompanied by an increase in its electron population and stability. If these are examples of what could be termed increases in *steric strain*, then such strain and its consequences must be sharply distinguished from the *geometric strain* found in small ring systems as described above. The two types of strain exhibit opposite behavior with respect to the volume change accompanying increases in the stability and electron population of a carbon atom.

This study of the properties of atoms in molecules shows that a carbon atom subjected to geometrical strain, an unsaturated carbon atom, and an sp^2 carbon in a carbocation exhibit similar properties with respect to changes in their atomic populations, energies, and volumes. For example, reactions leading to a reduction in geometric strain, in unsaturation, or in positive charge will all proceed at a faster rate with an increase in pressure, for all these reactions lead to a decrease in the volumes of the associated carbon atoms. (The atomic volume decrease associated with the loss of charge in a reaction of a carbocation could be offset to some extent by an accompanying decrease in the electroconstriction of a solvent.) Most important, a carbon atom subjected to an increasing degree of geometric strain behaves increasingly like an unsaturated carbon atom with respect to the paralleling behavior of its charge, stability, and volume. The hydrocarbons also demonstrate that the volumes of atoms and of functional groups can be a characteristic property, one that is transferable between systems. Future research will determine the volumes and

Table IV. Properties of Hydrogen-Bonded Dimers 6-31G**/6-31G**

$H_nAH\cdots BH_m$	E(RHF),[a] au	r(A···B), au	r(AH), au	∠AHB, deg	$\rho(r_c)$, au	$\nabla^2\rho(r_c)$, au	$\lvert r_c - r_H\rvert$[b]
$H_2NH\cdots NH_3$	−112.395 89	6.482	1.899	180.00	0.0122	0.0337	1.66
$HOH\cdots OH_2$	−152.056 06	5.633	1.791	171.32	0.0199	0.0624	1.34
$HOH\cdots NH_3$	−132.229 31	5.768	1.797	177.57	0.0214	0.0581	1.32
$H_3NH^+\cdots OH_2$	−132.603 46	5.203	1.955	179.88	0.0387	0.1370	1.05
$H_3NH^+\cdots NH_3$	−112.782 84	5.274	2.010	180.00	0.0507	0.1084	0.99
$H_2OH^+\cdots OH_2$	−152.387 93	4.525	2.042	177.32	0.1109	−0.0110	0.61
H_2O trimer	−228.085 95	5.669	1.786	153.08	0.0174	0.0539	
		5.732	1.788	163.22	0.0170	0.0536	

[a] The 6-31G**/6-31G** energies of the monomers, NH_3, NH_4^+, H_2O, and H_3O^+ are −56.195 54, −56.545 53, −76.023 62, and −76.310 32 au, respectively. [b] Distance of hydrogen bond critical point from proton.

their transferability of the four nucleic acids and of the functional groups appearing in proteins.

The tests of transferability proposed here are based on direct comparisons of the values of the properties of atoms in different molecules. More abstract definitions of transferability have also been proposed. Bertz and Herndon[37] have presented a definition of molecular similarity based upon the similarity of corresponding molecular graphs. The procedure involves the listing of all subgraphs of the molecular graph, the numbers of which form the basis for a set of similarity indexes. One of these indexes compares favorably with the standard distance measures of sequence comparison.

III. Atomic Volume Changes on Hydrogen-Bond Formation

This section presents a study of the changes in atomic volumes accompanying the formation of hydrogen bonds in the homo and hetero dimers of water and ammonia and in the corresponding protonated species. A water trimer is also studied. All calculations were done using the 6-31G** basis set at the corresponding optimized geometries. Previous theoretical results for the dimers with which the present results are in agreement are collected in references 38 to 42. Volume changes are reported for the 0.001-au envelope, but similar results are obtained using the 0.002-au envelope.

The total energies of the monomers and dimers together with pertinent geometrical information of the A—H···B fragment are presented in Table IV. The symbols A and B refer to the oxygen or nitrogen atom of the acid or base molecule and H to the atom shared in the hydrogen bond. The energy surface of the ammonia dimer is very flat with only a small difference in energy (less than 1 kcal/mol) between a linear C_s geometry reported here and a nearly cyclic structure.[40,42,43] The atomic properties of the two structures are very similar.

The energies of hydrogen-bond formation and the individual atomic contributions to these energy changes are given in Table V. In the neutral species, the strongest hydrogen bond is found in the mixed dimer, H_2O being a stronger acid than NH_3. The mixed dimer of the charged species is NH_4^+–H_2O. The stabilization of the base atom B dominates the energy changes for the charged systems, and this effect is greatest in the strongest of these interactions. Further discussion of the energy changes is given following the discussion of the changes in the atomic volumes and populations as given in Table VI. Table VI also gives the electron populations and volumes of the atoms in the monomers. The protonation of the N or O atoms in NH_3 or H_2O leads to an inductive transfer of charge from the hydrogen atoms and to an increase in the electron population of O or N. This observation is in accord with the increase in the ^{15}N chemical shift found to accompany protonation of ammonia or an amine.

Table V. Hydrogen-Bond Energies and Their Atomic Contributions[a]

$H_nAH\cdots BH_m$	ΔE[d]	ΔE-(acid)	ΔE-(base)	ΔE-(A)	ΔE-(H)	ΔE-(B)[c]
$H_2NH\cdots NH_3$	−3.0	−5.3	2.3	−14.8	20.9	−7.1
$HOH\cdots OH_2$	−5.5	−10.6	5.0	−23.5	16.4	−7.5
$HOH\cdots NH_3$	−6.4	2.7	−9.2	−12.4	21.4	−28.7
$H_3NH^+\cdots OH_2$	−21.5	−27.2	5.7	−31.4	33.5	−38.8
$H_3NH^+\cdots NH_3$	−26.2	−21.5	−4.4	−23.2	42.6	−75.7
$H_2OH^+\cdots OH_2$	−33.8	−15.0	−18.9	4.8	13.7	−93.4
H_2O trimer[b]	−9.5	−15.1	3.7	−37.0	8.1	−7.5
			1.8		13.8	−7.5

[a] In kcal/mol. [b] The H bond with the shorter O···O distance is listed first. [c] The symbols A and B refer to the oxygen or nitrogen atom of the acid or base molecule, and H refers to the atom shared in the hydrogen bond. [d] ΔE is the difference in the calculated SCF total energies. ΔE(acid) and ΔE(base) are the sums of the changes in the corresponding atomic energies as determined by numerical integration.[24] Thus there can be a small difference between ΔE and ΔE(acid) + ΔE(base). This error, resulting from the integration over an atomic basin to obtain an atomic property, is very small, being largest for the $NH_4^+\cdots NH_3$ dimer where it equals 0.3 kcal/mol.

The formation of a hydrogen bond is the result of an interaction between two closed-shell systems, and this is reflected in the properties of the charge distribution, particularly in its Laplacian, the quantity $\nabla^2\rho$.[44] The Laplacian of a scalar is an important quantity since it determines where the function is locally concentrated and locally depleted. When $\nabla^2\rho(r) < 0$ (>0) the value of the charge density at the point r is greater than (less than) the value of $\rho(r)$ averaged over all neighboring points in space. A maximum in $-\nabla^2\rho(r)$ means that electronic charge is locally concentrated in that region of space even though the charge density itself exhibits no corresponding maximum. Such maxima provide a faithful mapping of the number and positions of the bonded and nonbonded pairs of electrons assumed in the Lewis model.[45]

The interaction of two atoms leads to the formation of a (3, −1) critical point in the charge density, a point where $\nabla\rho = 0$ and where ρ has *three* curvatures, one positive and two negative, the sum of the signs of the curvatures equalling −1. The trajectories of $\nabla\rho$ associated with this critical point define the interatomic surface and the bond path.[17,44] This is illustrated in Figure 5 for the water dimer. The charge density is a maximum at the position of the critical point r_c in the interatomic surface, and hence charge is locally concentrated there as the two negative curvatures of ρ are perpendicular to the bond path. The charge density is a local minimum at r_c along the bond path as the third curvature is positive and charge is, therefore, locally depleted at the critical point with respect to neighboring points along the bond path. Thus the formation of an interatomic surface and a chemical bond is the result of a competition between the perpendicular contractions of ρ, which lead to concentration or compression of charge between the nuclei along the bond path, and the parallel expansion of ρ which leads to the separate concentration of charge in the basins of the neighboring atoms.

When $\nabla^2\rho(r_c) < 0$ and large in magnitude, the perpendicular contractions in ρ dominate the interaction and the result is a

(37) Bertz, S. H.; Herndon, W. C. *ACS Symp. Ser.* **1986**, No. 306, 1969.
(38) Frisch, M. J.; Del Bene, J. E.; Binkley, J. S.; Schaefer, H. F. *J. Chem. Phys.* **1986**, *84*, 2279.
(39) Kochanski, E. *Chem. Phys. Lett.* **1986**, *130*, 291.
(40) Hirao, E.; Fujikawa, T.; Konishi, H.; Yamabe, S. *Chem. Phys. Lett.* **1984**, *104*, 184.
(41) Frisch, M. J.; Pople, J. A.; Del Bene, J. E. *J. Phys. Chem.* **1985**, *89*, 3664.
(42) Latajka, Z.; Scheiner, S. *J. Chem. Phys.* **1986**, *84*, 341.
(43) Nelson, D. D., Jr.; Fraser, G. T.; Klemperer, W. *J. Chem. Phys.* **1985**, *83*, 6201. Fraser, G. T.; Nelson, D. D.; Charo, A.; Klemperer, W. *Ibid.* **1985**, *82*, 2535.
(44) Bader, R. F. W.; Essén, H. *J. Chem. Phys.* **1984**, *80*, 1943.
(45) Bader, R. F. W.; MacDougall, P. J.; Lau, C. D. H. *J. Am. Chem. Soc.* **1984**, *106*, 1594.

Table VI. Volume and Population[c] Changes for Hydrogen-Bond Formation

$H_nAH\cdots BH_m$	$-\Delta E$[a]	Δv[b]	Δv(acid)	Δv(base)	ΔN(acid) = $-\Delta N$(base)	Δv(A)	Δv(H)	Δv(B)	ΔN(A)	ΔN(H)	ΔN(B)
$H_2NH\cdots NH_3$	3.0	−5.17	−2.64	−2.53	0.009	0.82	−5.32	−1.57	0.032	−0.061	0.015
$HOH\cdots OH_2$	5.5	−10.65	−4.97	−5.67	0.012	1.18	−6.48	−3.90	0.045	−0.043	0.017
$HOH\cdots NH_3$	6.4	−12.06	−4.64	−7.43	0.022	1.55	−6.80	−4.57	0.054	−0.047	0.035
$H_3NH^+\cdots OH_2$	21.5	−16.11	−4.95	−11.16	0.033	1.44	−9.78	−4.85	0.040	−0.083	0.072
$H_3NH^+\cdots NH_3$	26.2	−19.97	−1.95	−18.01	0.081	2.08	−9.07	−7.59	0.050	−0.080	0.124
$H_2OH^+\cdots OH_2$	33.9	−25.06	−5.20	−19.86	0.096	−1.46	−6.18	−9.96	0.036	−0.009	0.079
H_2O trimer	9.5	−17.41	−8.32	−4.50	0.018	2.11	−4.81	−2.99	0.077	−0.022	0.016
				−4.58			−5.62	−3.21		−0.037	0.015

[a] ΔE in kcal/mol. [b] Δv in au using 0.001-au contour as envelope. [c] The atomic populations and volumes in the monomers are: $N(N) = 8.19$, $v(N) = 134.1$, $N(H) = 0.627$, $v(H) = 130.8$ in NH_3; $N(N) = 8.236$, $v(N) = 115.0$, $N(H) = 0.441$, $v(H) = 21.5$ in NH_4^+; $N(O) = 9.239$, $v(O) = 136.9$, $N(H) = 0.381$, $v(H) = 19.1$ in H_2O; $N(O) = 9.300$, $v(O) = 124.2$, $N(H) = 0.233$, $v(H) = 11.8$ in H_3O^+.

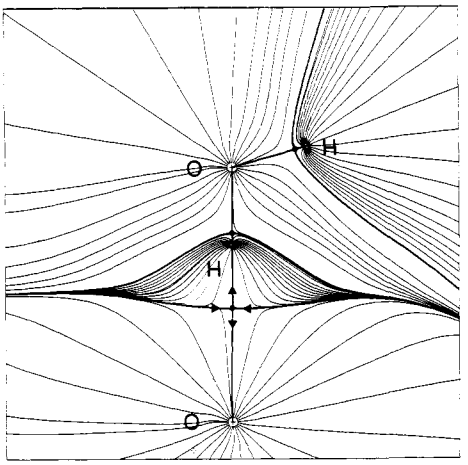

Figure 5. A representation of the gradient vector field for the hydrogen-bonded water dimer. Each line represents a trajectory traced out by a gradient vector of the charge density. The plane shown contains the three nuclei of the donor molecule. The two protons of the base molecule lie one above and one below this plane. A nucleus acts as an attractor of the $\nabla\rho$ field; i.e., all the trajectories in some open neighborhood of a nucleus, its associated basin, terminate at that nucleus. They are lines of steepest ascent through the charge density. An atom is the union of an attractor and its basin. Basins of neighboring atoms are separated by trajectories that terminate at a (3, −1) critical point (denoted by a black dot). In a symmetry plane a pair of such trajectories (shown as bold lines) terminate at each (3, −1) critical point. They denote the intersection of an interatomic surface with this plane. A pair of lines of steepest ascent (also shown as bold lines) originate at each (3, −1) critical point and terminate, one to each, at the neighboring nuclei. They define the atomic interaction lines—lines along which the charge density is a maximum with respect to any neighboring line. The directions of steepest ascent of the trajectories originating and terminating at the (3, −1) critical point of the hydrogen bond are indicated. The lack of a large curvature in the surface associated with the hydrogen bond is characteristic of such interactions.

sharing of electronic charge between the nuclei as is typical of covalent or polar covalent bonds. In this case the atoms are bound because of the lowering of the potential energy associated with the charge concentrated between the nuclei. Such behavior is, for example, found for the normal O–H and N–H bonds as illustrated in Figure 6 for O–H bonds which shows the Laplacian distributions for two hydrogen-bonded systems. Since charge is concentrated between the nuclei along the bond path, in these cases, the values of ρ and $|-\nabla^2\rho|$ at a bond critical point are relatively large, typical values being $\rho(r_c) = 0.358$ au, $\nabla^2\rho(r_c) = -1.938$ au for N–H in NH_3, and $\rho(r_c) = 0.391$ au, $\nabla^2\rho(r_c) = -2.443$ au for O–H in H_2O.

When $\nabla^2\rho(r_c) > 0$, one has the other limiting type of interaction, one dominated by the contraction of each atomic density toward its nucleus, resulting in a depletion of charge at the critical point and in the interatomic surface. These are called closed-shell interactions because they typify interactions between closed-shell atoms as found in noble gas repulsive states, ionic bonds, hydrogen bonds, van der Waals molecules, and the relatively long bonds found between what are formally closed-shell atoms in compounds such as S_4N_4 and S_8^{2+}. The relative depletion of charge in the interatomic surface of a closed-shell system (see Table IV for values of $\rho(r_c)$) is a consequence of the requirements of the Pauli exclusion principle. In these interactions the charge concentrations and the corresponding regions of excess potential energy are separately localized in the basins of the neighboring atoms.[44] Since these charge concentrations can be polarized into the bonded or nonbonded regions of the basins of the individual atoms, closed-shell interactions can give rise to bound or unbound states, respectively. In an ionic interaction both ions are polarized in a direction counter to the direction of charge transfer, as required for electrostatic equilibrium. The anionic nucleus experiences a net repulsive force from the cation, and thus the density of the anion polarizes into its bonded region to counterbalance this. The cationic nucleus, on the other hand, experiences a net force of attraction from the anion and hence the density of the cation must polarize into its nonbonded region to counterbalance it. Thus as a result of the charge transfer and resulting polarizations, both nuclei in an ionic molecule are bound by the charge density localized on the anion.

A hydrogen bond exhibits the characteristics of a closed-shell interaction. The values of the charge density at the critical point of the hydrogen bond, while paralleling the increase in hydrogen bond strength,[46] are all relatively small, Table IV. The corresponding value of the Laplacian is positive in all cases but that of the largest interaction in the series, that between hydronium ion and water. Appeal to Figure 6 shows that as the hydrogen-bond energy increases and the A–B separation undergoes a general decrease, the critical point of the hydrogen bond moves progressively closer to the zero contour encompassing the valence shell of charge concentration in the Laplacian distribution of the acid. In the H_3O^+–H_2O system the critical point lies just inside this contour.

The formation of a hydrogen bond is accompanied by a transfer of charge from the base to the acid, the magnitude of the transfer paralleling the increase in the strength of the interaction as shown by the data in Table VI. The magnitude of this transfer is relatively small compared to the changes in the individual atomic charges for the neutral dimers. There is, therefore, a considerable redistribution of charge within the acid and the base. The hydrogen-bonded atom H of the acid undergoes a loss in charge larger than or comparable to the total charge transferred between the base and acid, the only exception being found for the acidic hydrogen in the hydronium ion complex. This latter behavior is understandable in light of the large net positive charge already present on the hydrogens of the free hydronium ion. The largest fraction of the charge increase on the AH_n fragment of the acid resides on the A atom in the electrically neutral systems and on the nonparticipating hydrogens in the charged systems.

The net negative charge on the B atom of the base BH_m increases in magnitude on the formation of a hydrogen bond by an amount which, in general, is greater than the total electronic charge lost by the base. Thus the m hydrogen atoms of the base undergo both intra- and intermolecular charge transfer, trans-

(46) Boyd and Choi have previously noted a strong correlation of $\rho(r_c)$ of the bond critical point and the energy of a hydrogen bond: Boyd, R. J.; Choi, S. C. *Chem. Phys. Lett.* **1985**, *120*, 80; **1986**, *129*, 62.

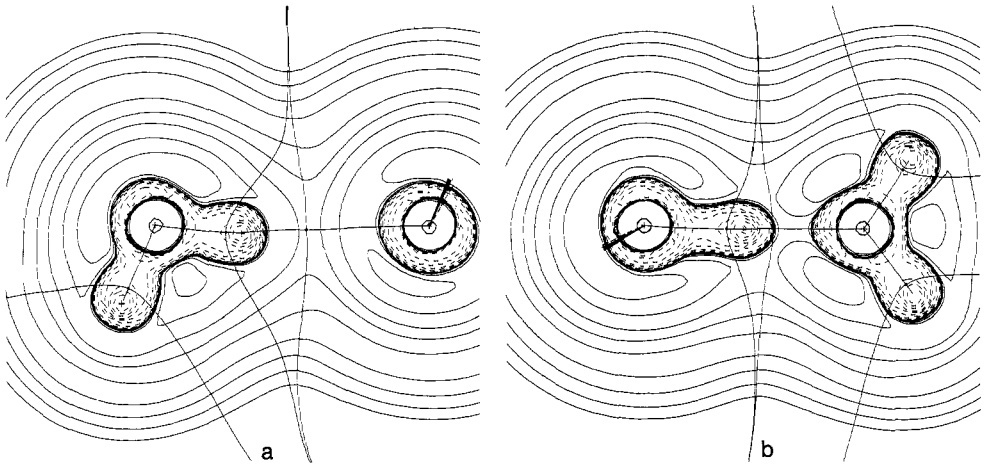

Figure 6. Contour maps of the Laplacian distribution of the electronic charge density for HO—H···OH_2 (a) and $[H_2O—H···OH_2]^+$ (b). The out-of-plane hydrogens of the base in (a) and of the acid in (b) are indicated. Solid contours denote positive values of $\nabla^2\rho$, regions of charge depletion, and dashed contours denote negative values of $\nabla^2\rho$, regions of charge accumulation. The interatomic surfaces and bond paths are also shown. The critical point of the hydrogen bond in the charged complex is found just inside the zero contour encompassing the proton and the bond has some of the characteristics of a shared interaction.

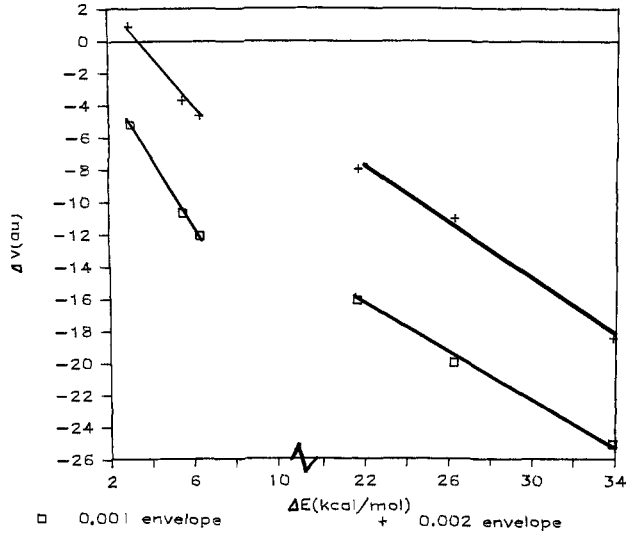

Figure 7. Plots of ΔV versus ΔE of hydrogen-bond formation for the dimers listed in Table VI. The volume changes, V(dimer) − V(monomers), in the upper curves are determined using the 0.002-au envelope, while those in the lower curves are the 0.001-au envelope of the density.

ferring charge to the B atom of the base as well as to the acid.

There is a decrease in the molecular volumes of both reactants upon formation of a hydrogen bond, the magnitude of the total decrease paralleling the strength of the interaction as illustrated in Figure 7. The two sets of nearly linear data points lead to energy changes per unit change in volume of 0.54 and 1.33 kcal/a_0^3 for the neutral and charged dimers, respectively. The largest atomic decreases in volume are for the H atom of the acid and for the B atom of the base, a result of the formation of a new interatomic surface between these two atoms. Reference to Figures 5 and 6 shows that the new interatomic surface formed between the B and H atoms is much flatter than is that for a normal O–H or N–H bond. The critical point of the hydrogen bond is also further removed from the proton than it is in the A–H bond of the acid. This is a general result and is true for B and A equal to N, O, or F. The formation of the hydrogen bond causes the A–H bond critical point to move closer to the proton by 0.02 to 0.04 au. The distance of the hydrogen-bond critical point from this proton decreases as the hydrogen bond energy increases (Table IV), and both of these effects lead to decreases in v(H). The magnitude of the latter decrease parallels the strength of the interaction. The decrease in the H-atom volume is relatively small for the final member, the H_3O^+–H_2O system, a result of the very contracted nature of the charge distribution in the hydronium ion.

The charge and volume changes for a water trimer wherein a single water molecule provides both acidic hydrogens are also given in Table VI. The formation of the water dimer results in an energy lowering of 5.5 kcal/mol, and the formation of a second hydrogen bond lowers the energy by another 3.9 kcal/mol. The energy and volume decrease on dimer formation are both ~60% of that observed for the formation of the trimer. Each H atom of the acid undergoes a loss of electronic charge and volume on hydrogen bonding, greater than one-half of that found in the formation of the dimer. The base atoms B undergo increases in electronic charge and decreases in energy almost identical with those found for the formation of the dimer. The decreases in their volumes are about three-quarters as great. The increases in charge, stability, and volume found for the oxygen atom of the acid are almost twice as large as those found for the dimer.

Changes in atomic volumes accompanying a chemical reaction can be calculated and are found, along with changes in atomic populations and energies, to be characteristic of a given reaction. In the formation of a hydrogen bond the hydrogen-bonded atom H undergoes a decrease in electronic charge, stability, and volume. The B atom of the base undergoes an increase in electronic charge and stability, but its volume also decreases as a result of the formation of a bond and the associated interatomic surface with the H atom. The charge and energy changes for the H and B atoms are as anticipated for an interaction which is basically ionic in nature. The substantial initial net charges on the hydrogen-bonded H atom and the base atom B are further increased, and the accompanying polarizations of the base and acid molecules are in a direction counter to the direction of this apparent charge transfer. The charge transferred to the base atom B lowers the energy of the system and is the major source of stability in the tightly bound systems. It is the same transfer of charge to atom B which binds both nuclei in an ionic system in the electrostatic interpretation of binding using the Hellmann–Feynman theorem.

The ability to determine the individual atomic contributions to the changes in charge, energy, and volume characteristic of a given chemical reaction should be of particular use in obtaining a better understanding of the atomic interactions between large biological molecules. A study of the hydrogen-bonded interactions leading to the base pairs present in DNA is to be initiated in this laboratory. The information made possible through the quantum mechanical description of the properties of an atom in a molecule and the changes in these properties upon reaction would clearly be of particular use in the study of the mechanism of energy storage and its release in molecules such as ATP.

Acknowledgement is made to the donors of the Petroleum Research Fund, administered by the American Chemical Society,

for partial support of this research.

Registry No. NH_3, 7664-41-7; H_2O, 7732-18-5; C_2H_6, 74-84-0; C_3H_8, 74-98-6; C_4H_{10}, 106-97-8; C_5H_{12}, 109-66-0; C_6H_{14}, 110-54-3; *iso*-C_4H_{10}, 75-28-5; *neo*-C_5H_{12}, 463-82-1; H_2, 1333-74-0; N_2, 7727-37-9; O_2, 7782-44-7; Ne, 7440-01-9; Ar, 7440-37-1; NO, 10102-43-9; HF, 7664-39-3; CO, 630-08-0; PH_3, 7803-51-2; F_2, 7782-41-4; CO_2, 124-38-9; SO_2, 7446-09-5; NO_2, 10024-97-2; HCN, 74-90-8; HCP, 6829-52-3; HCl, 7647-01-0; C_4H_8, 287-23-0; C_6H_{12}, 110-82-7; CH_3^+, 14531-53-4; $C_4H_9^+$, 25453-90-1; C_2H_4, 74-85-1; C_2H_2, 74-86-2; C, 7440-44-0; cyclopropane, 75-19-4; cyclohexane, 110-82-7; methane, 74-82-8; bicyclo[1.1.0]butane, 157-33-5; [1.1.1]-propellane, 311-75-1.

Metal, Bond Energy, and Ancillary Ligand Effects on Actinide–Carbon σ-Bond Hydrogenolysis. A Kinetic and Mechanistic Study

Zerong Lin and Tobin J. Marks*

Contribution from the Department of Chemistry, Northwestern University, Evanston, Illinois 60201. *Received January 20, 1987*

Abstract: A kinetic/mechanistic study of actinide hydrocarbyl ligand hydrogenolysis (An–R + H_2 → An–H + RH) is reported. For the complex $Cp'_2Th(CH_2\text{-}t\text{-}Bu)(O\text{-}t\text{-}Bu)$ ($Cp' = \eta^5\text{-}Me_5C_5$), the rate law is first-order in organoactinide and first-order in H_2, with $k_{H_2}/k_{D_2} = 2.5$ (4) and $k_{THF}/k_{toluene} = 2.9$ (4). For a series of complexes, hydrogenolysis rates span a range of ca. 10^5 with $Cp'_2\overbrace{ThCH_2C(CH_3)_2}CH_2 \approx Cp'_2U(CH_2\text{-}t\text{-}Bu)(O\text{-}t\text{-}Bu)$ (too rapid to measure accurately) > $Cp'_2Th(CH_2\text{-}t\text{-}Bu)[OCH(t\text{-}Bu)_2] = Cp'_2Th(CH_2\text{-}t\text{-}Bu)(O\text{-}t\text{-}Bu) > Cp'_2Th(CH_2\text{-}t\text{-}Bu)(Cl) > Me_2Si(Me_4C_5)_2Th(n\text{-}Bu)_2 > Cp'_2Th(n\text{-}Bu)_2 \approx Cp'_2ThMe_2 > Cp'_2Th(Me)(O_3SCF_3) > Cp'_2Th(n\text{-}Bu)[OCH(t\text{-}Bu)_2] \approx Cp'_2Th(Me)[OSiMe_2(t\text{-}Bu)] > Cp'_2ZrMe_2 = Cp'_2Th(p\text{-}C_6H_4NMe_2)(O\text{-}t\text{-}Bu) > Cp'_2Th(Ph)(O\text{-}t\text{-}Bu) > Cp'_2U(Me)[OCH(t\text{-}Bu)_2] > Cp'_2Th(Me)[OCH(t\text{-}Bu)_2]$. In the majority of cases, the rate law is cleanly first-order in organoactinide over 3 or more half-lives. However, for Cp'_2ThMe_2 → $(Cp'_2ThH_2)_2$, an intermediate is observed by NMR that is probably $[Cp'_2Th(Me)(\mu\text{-}H)]_2$. For $Cp'_2Th(Me)(O_3SCF_3)$, a follow-up reaction, which consumes $Cp'_2Th(H)(O_3SCF_3)$, is detected. Variable-temperature kinetic studies yield $\Delta H^\ddagger$ = 3.7 (2) kcal/mol and $\Delta S^\ddagger = -50.8$ (7) eu for $Cp'_2Th(CH_2\text{-}t\text{-}Bu)(O\text{-}t\text{-}Bu)$ and $\Delta H^\ddagger = 9$ (2) kcal/mol and $\Delta S^\ddagger = -45$ (5) eu for $Cp'_2U(Me)[OCH(O\text{-}t\text{-}Bu)_2]$. The present results are in accord with a polar "heterolytic" four-center transition state involving significant H–H bond cleavage. There is no chemical shift or spin–lattice relaxation time NMR spectroscopic evidence for an H_2 complex in preequilibrium. There are approximate correlations between the hydrogenolysis rate and An–R bond disruption enthalpy, ancillary ligand electron-donor capacity, and An–R migratory CO insertion rate. Possible parallels between the present results and the activities of supported organoactinide catalysts, as well as the mechanism of molecular weight control by hydrogen in Ziegler-Natta catalysis, can be drawn.

Processes by which metal–carbon σ bonds suffer hydrogenolysis are essential components of numerous catalytic cycles.[1] For early-transition-metal, lanthanide, and actinide systems, many mechanistic aspects of the hydrogenolysis process remain obscure, despite the importance of such transformations in olefin and alkyne hydrogenation catalysis,[2–4] as well as in molecular weight control during coordination polymerization.[5] Additional motivation to better understand H–H activation processes in d^0/f^0 systems is provided by the possibility of more effectively modulating analogous C–H functionalization processes.[6–8] Mechanistically, the absence of energetically accessible metal oxidation states for oxidative addition/reductive elimination processes,[1,9] the presence of relatively low-lying empty metal σ-bonding orbitals, and the

(1) For examples in homogeneous solution, see: (a) Collman, J. P.; Hegedus, L. S.; Norton, J. R.; Finke, R. G. *Principles and Applications of Organotransition Metal Chemistry*; University Science Books: Mill Valey, CA, 1987; Chapter 10. (b) James, B. R. In *Comprehensive Organometallic Chemistry*; Wilkinson, G., Stone, F. G. A., Abel, E. W., Eds.; Pergamon: Oxford, 1982; Chapter 51. (c) Masters, C. *Homogeneous Transition-metal Catalysis*; Chapman and Hall: London, 1981; Chapter 2.1. (d) Parshall, G. W. *Homogeneous Catalysis*; Wiley-Interscience: New York, 1980; Chapter 3. (e) Crabtree, R. *Acc. Chem. Res.* **1979**, *12*, 331–338, and references therein.

(2) Early transition metals: (a) Couturier, S.; Tainturier, G.; Gautheron, G. *J. Organomet. Chem.* **1980**, *195*, 291–306. (b) Wailes, P. C.; Weigold, H.; Bell, A. P. *J. Organomet. Chem.* **1972**, *43*, C32–C34.

(3) Lanthanides: (a) Jeske, G.; Lauke, H.; Mauermann, H.; Schumann, H.; Marks, T. J. *J. Am. Chem. Soc.* **1985**, *107*, 8111–8118. (b) Mauermann, H.; Swepston, P. N.; Marks, T. J. *Organometallics* **1985**, *4*, 200–202. (c) Evans, W. J.; Bloom, I.; Hunter, W. E.; Atwood, J. L. *J. Am. Chem. Soc.* **1983**, *105*, 1401–1403.

(4) Actinides: (a) Marks, T. J. In *The Chemistry of the Actinide Elements*; 2nd ed.; Katz, J. J., Seaborg, G. T., Morss, L. R., Eds.; Chapman and Hall: London, 1986; Chapter 23. (b) Marks, T. J.; Day, V. W. In *Fundamental and Technological Aspects of Organo-f-Element Chemistry*; Marks, T. J., Fragalà, I. L., Eds.; Reidel: Dordrecht, 1985; Chapter 4. (c) Fagan, P. J.; Manriquez, J. M.; Maata, E. A.; Seyam, A. M.; Marks, T. J. *J. Am. Chem. Soc.* **1981**, *103*, 6650–6667. (d) Duttera, M. R.; Mauermann, H.; Marks, T. J., unpublished results quoted in ref 3a.

(5) (a) Quirk, R. P., Hsieh, H. L., Klingensmith, G. B., Tait, P. J., Eds. *Transition Metal Catalyzed Polymerization. Alkenes and Dienes*; Harwood Publishers for MMI Press: New York, 1983. (b) Gavens, P. D.; Bottrill, M.; Kelland, J. W.; McMeeking, J. In reference 1a, Chapter 22.5. (c) Boor, J., Jr. *Ziegler-Natta Catalysts and Polymerizations*; Academic: New York, 1979; pp 251–256.

(6) Early transition metals: (a) Rothwell, I. P. *Polyhedron* **1985**, *4*, 177–200. (b) Thompson, M. E.; Bercaw, J. E. *Pure Appl. Chem.* **1984**, *56*, 1–11. (c) Thompson, M. E.; Baxter, S. M.; Bulls, A. R.; Burger, B. J.; Nolan, M. C.; Santarsiero, B. D.; Schaefer, W. P.; Bercaw, J. E. *J. Am. Chem. Soc.* **1987**, *109*, 203–219.

(7) Lanthanides: (a) Watson, P. J.; Parshall, G. W. *Acc. Chem. Res.* **1985**, *18*, 51–56. (b) Jeske, G.; Lauke, H.; Mauermann, H.; Sweptson, P. J.; Schumann, H.; Marks, T. J. *J. Am. Chem. Soc.* **1985**, *107*, 8091–8103. (c) Jeske, G.; Schock, L. E.; Swepston, P. J.; Schumann, H.; Marks, T. J. *J. Am. Chem. Soc.* **1985**, *107*, 8103–8110.

(8) Actinides: (a) Simpson, S. J.; Andersen, R. A. *J. Am. Chem. Soc.* **1981**, *103*, 4064–4066. (b) Bruno, J. W.; Marks, T. J.; Day, V. W. *J. Am. Chem. Soc.* **1982**, *104*, 7357–7360. (c) Bruno, J. W.; Smith, G. M.; Marks, T. J.; Fair, C. K.; Schultz, A. J.; Williams, J. M. *J. Am. Chem. Soc.* **1986**, *108*, 40–56. (d) Fendrick, C. M.; Marks, T. J. *J. Am. Chem. Soc.* **1984**, *106*, 2214–2216. (e) Fendrick, C. M.; Marks, T. J. *J. Am. Chem. Soc.* **1986**, *108*, 425–437. (f) Smith, G. M.; Carpenter, J. D.; Marks, T. J. *J. Am. Chem. Soc.* **1986**, *108*, 6805–6807.

(9) (a) Saillard, J.-Y.; Hoffmann, R. *J. Am. Chem. Soc.* **1984**, *106*, 2006–2026. (b) Reamey, R. H.; Whitesides, G. M. *J. Am. Chem. Soc.* **1984**, *106*, 81–85. (c) Crabtree, R. H.; Hlatky, G. *Inorg. Chem.* **1980**, *19*, 572–574.

0002-7863/87/1509-7979$01.50/0